

Automotive USB 2.0 and a 5 V, Type-C Solution for Charging and Robust Data Line Protection

Tao Tao, Senior Applications Engineer
and Trevor Crane, Senior Design Engineer

Introduction

USB charging ports have become an essential part of the modern vehicle infotainment system. Passengers are increasingly accustomed to connecting their vehicle's electrical system to both power their smartphones (or other portable devices) and, conversely, use those devices for a variety of vehicle information and entertainment functions. To support both power and data capabilities, and to enable adaptability in continuously fast-changing portable device markets, USB charging ports must meet a variety of system requirements with respect to power, data transmission, and robustness in the face of real-world hazardous events.

Portable device battery charging—including the ability to support a wide variety of device charger profiles such as USB BC 1.2 charging downstream port (CDP), dedicated charging port (DCP), standard downstream port (SDP), and common proprietary profiles—is only one part of a wide range of demands placed on USB charging ports. Other requirements include maintenance of signal integrity for high speed USB data transmission, and USB host protection from hazardous conditions commonly found in the automotive environment. In addition, small

solution size and low electromagnetic emissions are important requirements for meeting the demands of increasingly complex automotive electronics. This article demonstrates a solution that satisfies the requirements of modern USB charging ports in the automotive environment, including design examples.

Overview of an Automotive USB Power System

Figure 1 shows a block diagram of a typical automotive USB charger system, in which a switching regulator generates 5 V from the battery to power V_{BUS} . The USB charging port emulator plus power switch IC shown here has three main functions. First, the USB charging port emulator determines an attached device's optimal charging current, enabling fast charging via charging port modes such as USB BC 1.2 CDP, DCP, and vendor-proprietary charger emulation profiles. Second, the USB power switch acts as a current limiter and switch, sensing and limiting the bus current. Finally, the port controller supports USB 2.0 high speed data transfer between an attached device and the USB host.

Since USB ports exist in a harsh automotive environment, sensitive USB circuits must be protected from a host of real-world hazards, such as electrostatic

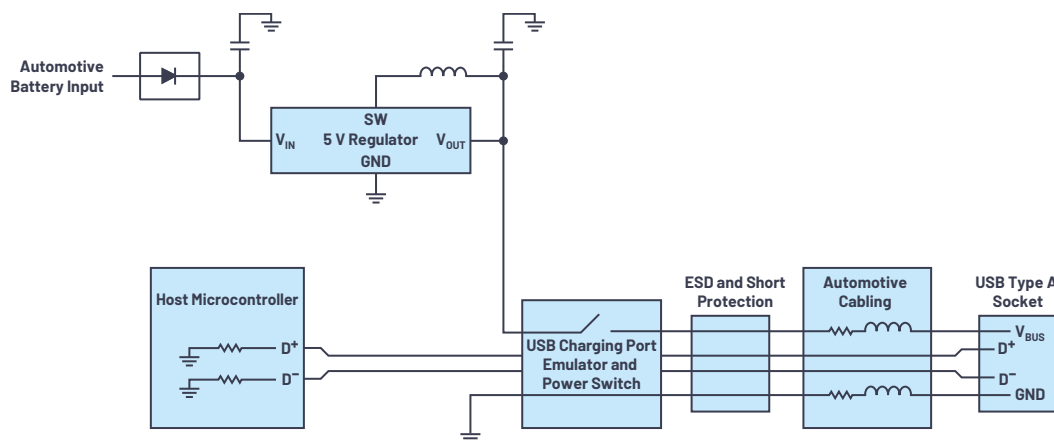


Figure 1. Automotive USB charger block diagram.

discharge (ESD) events at the socket and cable fault events, which can expose affected wiring to voltages well beyond their normal operating values.

Figure 2 shows a simplified block diagram of an automotive USB power system that combines many of the power, port, and protection functions into a single IC. In this case, the **LT8698S** integrates the functions of the switching regulator and power switch into a 4 mm × 6 mm package while providing robust data line protections against ESD events and cable faults.

With the integrated charger solution shown, all of the necessary hardware to independently perform the USB BC 1.2 CDP negotiation sequence between the USB port and the portable device is included, allowing CDP compliant devices to draw current up to 1.5 A from V_{BUS} while simultaneously communicating with the host at high speed.

Cable Drop Compensation

Cable drop compensation maintains accurate 5 V regulation of the V_{BUS} rail when the USB socket is physically distant from the controller—for instance, the USB socket is located in the rear of a vehicle and the USB host is in the dash. The **LT8698S** features programmable cable drop compensation to provide excellent regulation at the USB socket without the need for additional Kelvin sense wires.

Figure 3 shows how cable drop compensation works. A sense resistor, R_{SEN} , is tied between the OUT/ISP and BUS/ISN pins in series between the regulator output and the load. The **LT8698S** develops a current source value of $46 \times (V_{OUT/ISP} - V_{BUS/ISN})/R_{CBL}$ at its R_{CBL} pin through the R_{CBL} resistor to ground. This current is identical to the current flowing into the USB5V pin through the R_{CDC} resistor tied between the regulator output and the USB5V pin. This creates a voltage offset across the R_{CDC} resistor, above the 5 V USB5V feedback pin, and proportional to the R_{CDC}/R_{CBL} resistor ratio. As a result, the **LT8698S** regulates the BUS/ISN pin to a point, in proportion to the load current, above the at-the-load target 5 V (subject to a max limit of 6.05 V) to maintain accurate regulation at the socket's V_{BUS} pin.

Cable drop compensation eliminates the need to run an additional pair of Kelvin sense wires from the regulator to the remote load, but requires the system designer to know the cable resistance, R_{CABLE} —the **LT8698S** does not sense this value. Components for programming the cable drop compensation can be chosen using the following equation: $R_{CBL} = 46 \times R_{SEN} \times R_{CDC}/R_{CABLE}$. Since cable resistance varies with temperature, to achieve better overall output voltage accuracy over a wide temperature range, cable drop compensation can be made to vary vs. temperature by adding a negative temperature coefficient (NTC) resistor as part of R_{CBL} .

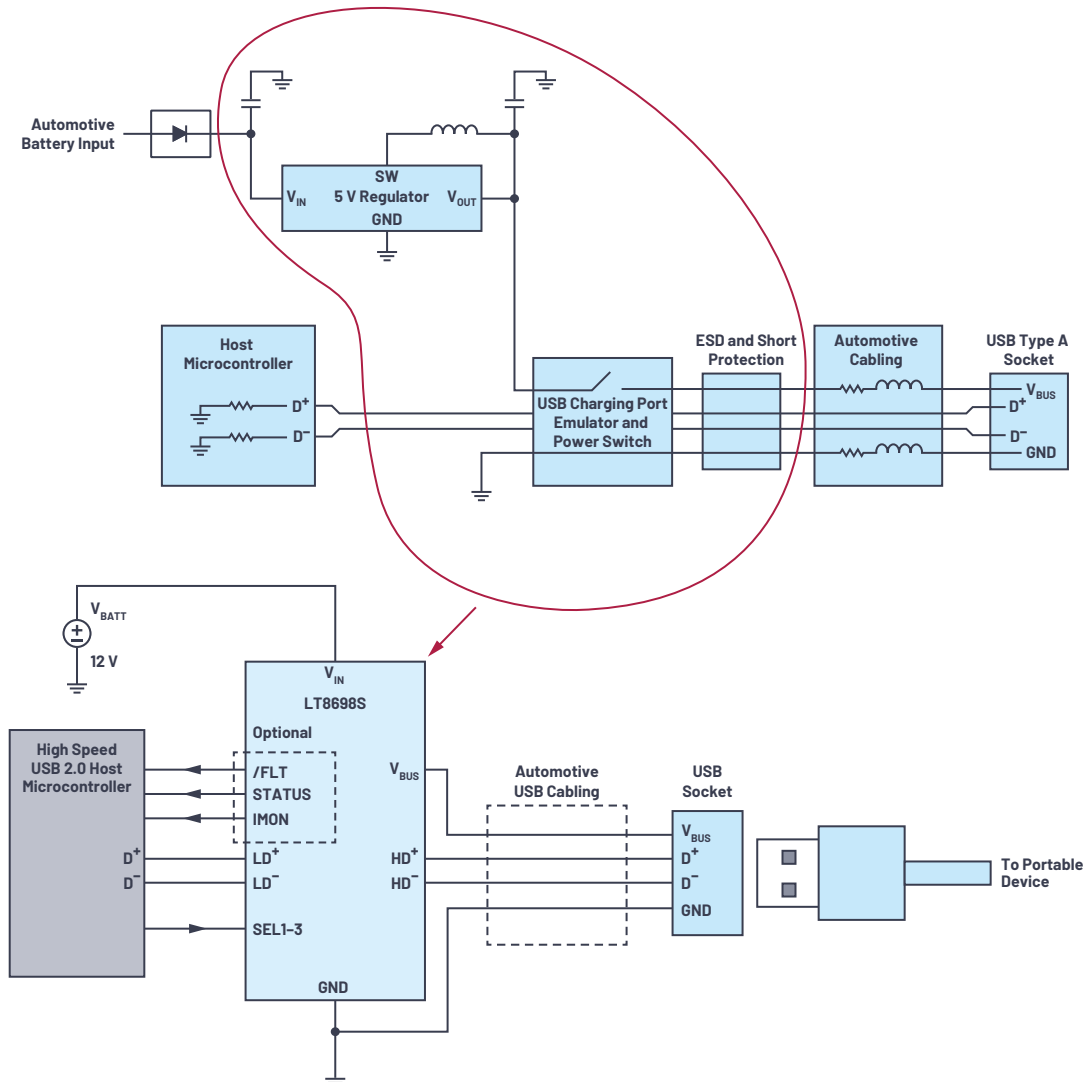


Figure 2. Simplified block diagram of an automotive USB power system built around a single-IC USB controller solution.

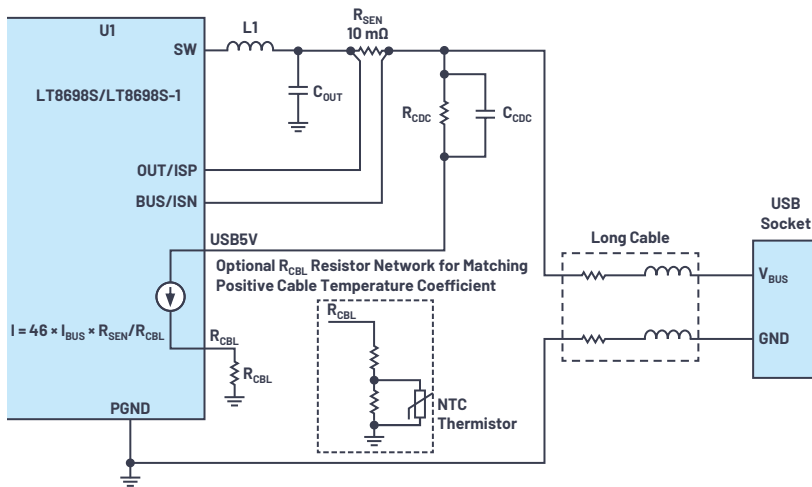


Figure 3. Working principles of cable drop compensation.

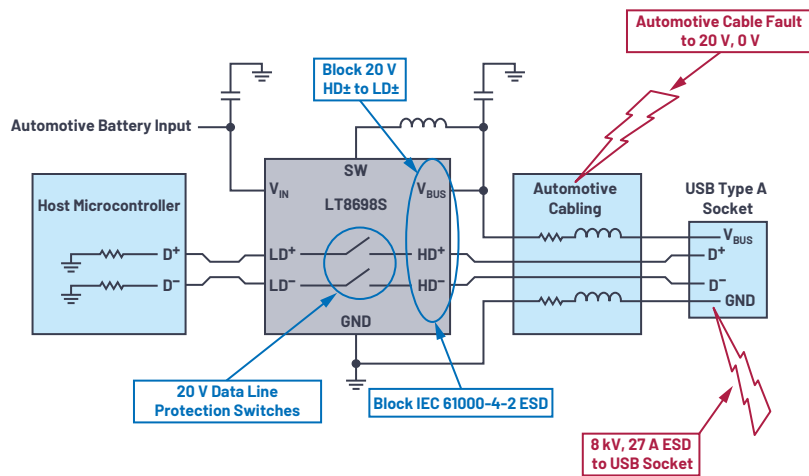


Figure 4. Robust protection features of LT8698S/LT8698S-1.

Robust Protection for Automotive Environment

The automotive environment presents a number of hazards from which the USB host must be protected. These hazards include cable faults resulting in data line exposure to the battery voltage or ground, and large ESD strikes at the USB socket. Figure 4 shows how to protect the USB host from these hazards.

The LT8698S's HD⁺ and HD⁻ pins withstand up to 20 V_{DC} and block up to 8 kV contact discharge and 15 kV air discharge IEC 61000-4-2 ESD events while simultaneously protecting the host from these severe conditions. In addition, the USB5V, OUT/ISP, and BUS/ISN pins withstand output voltage faults that include dc voltages up to 42 V. In the event of an output fault, the latch-off and auto-retry features accurately limit the average output current.

While many USB port controller ICs require external clamp diodes or capacitors on the data lines for ESD protection—increasing cost and material, while possibly degrading signal integrity—the LT8698S does not.

Despite the data line switches' ability to withstand dc faults and ESD events as previously stated, they also support excellent signal integrity. Specifically, the -3 dB bandwidth of the HD⁺ and HD⁻ pins is 480 MHz (typ), which is production tested. Figure 5 shows the high speed transmit eye pattern measured on a

demo board at test plane 2 in accordance with the USB 2.0 specification. This diagram shows conformance to USB template 1, test plane 2 limits with plenty of margin.

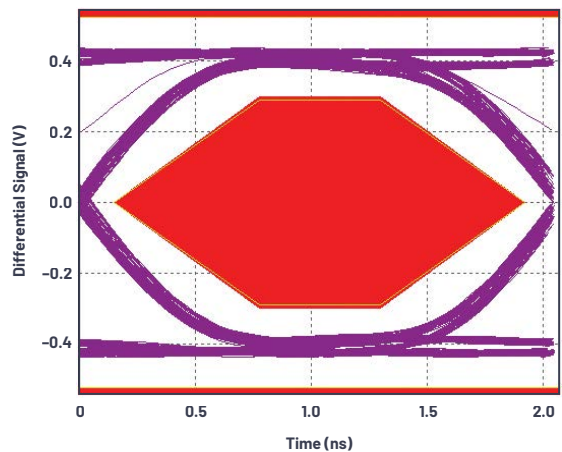


Figure 5. High speed USB 2.0 eye diagram measured on a demo board. Template 1 requirements shown.

Compatibility and Support for Wide Variety of Charger Profiles

The controller IC used in the examples here is compatible with a number of USB connector types and charger profiles as shown in Table 1. Let's look at how a single controller solution might work in a USB type-C 5 V, 3 A solution (15 W).

Figure 6 shows the schematic for a USB 5 V at 3 A V_{BUS} regulator with cable drop compensation. In this circuit, the R_{SEN} resistor value of 8 m Ω is chosen to support up to 3 A of current, and the SYNC/MODE pin is tied to ground to enable pulse-skipping mode of operation, reducing the switching frequency and quiescent current at light load currents.

The LT8698S also supports USB BC 1.2 DCP mode, which can supply charging currents up to 1.5 A for high current charging capability. When used as a DCP port, the D^+ and D^- lines are shorted together and there is no data transfer.

Many portable device manufacturers have developed proprietary charger protocols. In addition, these vendor-proprietary charger profiles and associated maximum charge currents, such as 2.0 A, 2.4 A, 2.1 A, and 1.0 A, are supported. The host microcontroller can implement these charger profiles by controlling the three SEL pins.

Figure 7 shows the schematic for a 2.4 A/1.5 A USB charger. In this application, the microcontroller utilizes the information provided by the LT8698S STATUS pin and IMON current monitor to select the desired charger profile by controlling the SEL1-3 pin input pins. In this way, the microcontroller can optimize the charger profile to the portable device for safe charging at the highest possible current.

Table 1. LT8698S/LT8698S-1 Compatibility to Wide Variety of USB Connector Types, Charger Profiles, and Data Interfaces

USB 2.0 Type-A		USB 3.x Type-A		USB Type-C	
Pins:	V_{BUS} , GND, D^+ , D^-	Pins:	V_{BUS} , GND, D^+ , D^-	Pins:	V_{BUS} , GND, D^+ , D^-
Power:	5 V, 1.5 A, BC 1.2 5 V, 2.4 A, Apple iPad	Power:	5 V, 1.5 A, BC 1.2	Power:	5 V, 1.5 A, BC 1.2 5 V, 3 A, type-C
Data:	USB 2.0, 480 Mbps	Data:	USB 2.0, 480 Mbps	Data:	USB 2.0, 480 Mbps

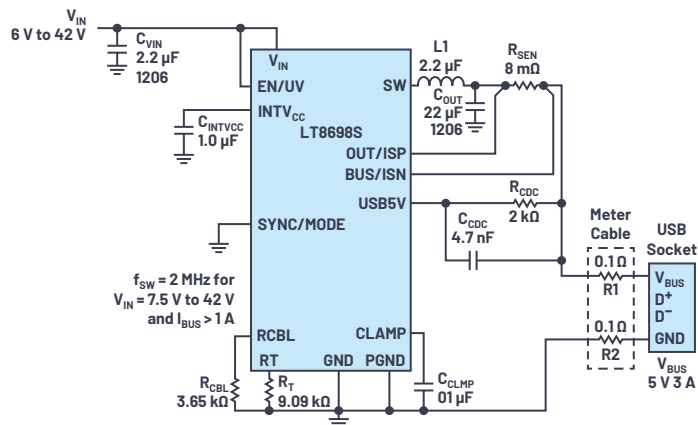


Figure 6. A 5 V, 3 A, USB type-C application.

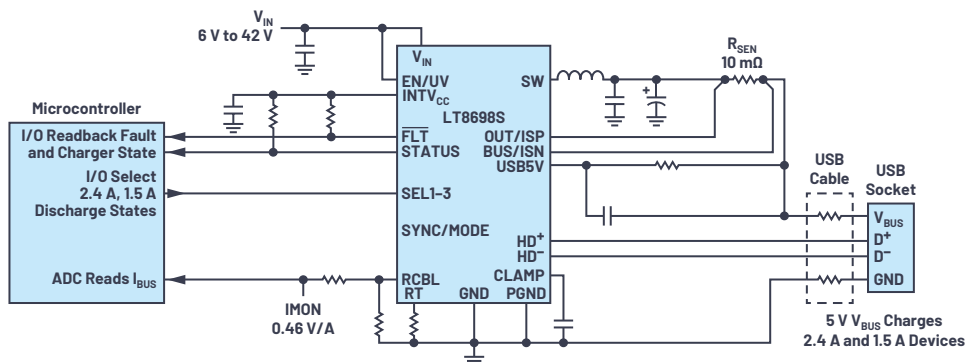


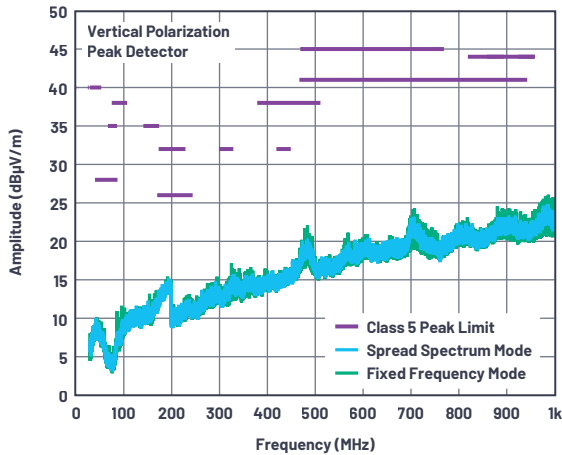
Figure 7. A 2.4 A/1.5 A automatic profile detection charger with current monitor.

EMI Solution

Low EMI is a key requirement for power supplies in automotive electronics systems, which are often expected to meet the CISPR 25 Class 5 emissions standard. The LT8698S is designed using Silent Switcher[®] 2 technology, enabling the USB power supply to meet these stringent automotive EMI standards without sacrificing solution size, efficiency, and robustness.

The Silent Switcher 2 architecture incorporates internal bypass capacitors configured for minimal EMI inside the LQFN package. The integration of the bypass capacitors simplifies board design and reduces the overall solution footprint while minimizing the effect of PCB layout on EMI performance. The LT8698S-1 does not include these internal bypass capacitors but is otherwise identical to the LT8698S. Selectable spread spectrum frequency modulation is also available in both devices by applying a dc voltage above 3.0 V to the SYNC/MODE pin. Figure 8 shows the radiated EMI performance of the LT8698S under typical application conditions.

The LT8698S and LT8698S-1 can operate with a programmable and synchronizable switching frequency in the range of 300 kHz to 3 MHz. Higher switching frequencies allow smaller inductor and capacitor values for smaller total solution size. Figure 9 shows that even at a relatively high switching frequency of 2 MHz, this 12 V to 5 V USB solution achieves 93% efficiency.



DC2688A-A Demo Board (with EMI Filter Installed)
14 V Input to 5 V_{BUS} Output at 2.5 A, $f_{SW} = 2$ MHz
L1 = XFL4020-222ME, C_{VIN2} and C_{VIN3} Populated

Figure 8. Radiated EMI performance (CISPR 25 radiated emissions with peak detector and Class 5 peak limit).



Figure 9. Efficiency and power loss curves for a 5 V USB solution.

Conclusion

USB charging ports, an essential part of the modern vehicle infotainment system, must negotiate a variety of system challenges with respect to power, data transmission support, and robustness in the face of real-world hazardous events expected in the automotive environment. The examples shown here, using the LT8698S USB charger IC, address these challenges. They support a wide variety of portable device charger profiles and can provide up to 15 W of output power for USB type-C charging applications. Additionally, they protect the USB host from potentially hazardous conditions such as cable faults and severe ESD events. The LT8698S provides this protection while maintaining the signal integrity necessary for high speed USB data transfer between the USB host and the portable device. Finally, Silent Switcher 2 architecture provides excellent EMI performance without sacrificing efficiency and solution size.



About the Author

Tao Tao is a senior applications engineer for power products at Analog Devices, Inc., in Santa Clara, California. He currently provides applications support for step-down switching regulator ICs. Prior to his current role, Tao worked at Intersil Corporation on developing integrated power modules. Tao's interests include high efficiency and high density power converters and regulators, modeling and control of power converters, EMI mitigation techniques, electronic packaging technologies, PCB board design, and solving any other technical problems. Tao obtained a master's degree in electrical engineering from Virginia Polytechnic Institute and State University, Blacksburg, Virginia. He can be reached at tao.tao@analog.com.



About the Author

Trevor Crane is a senior design engineer at ADI. He currently works for ADI's Power Business Unit at the Grass Valley location designing multichannel buck regulators. He graduated in 2004 from Stanford University with a B.S. in electrical engineering. Trevor has previously held roles at Linear Technology Corp. as a product engineer and as a design engineer working on discrete power products. He has released three automotive USB buck regulators. He can be reached at trevor.crane@analog.com.



AHEAD OF WHAT'S POSSIBLE™

For regional headquarters, sales, and distributors or to contact customer service and technical support, visit analog.com/contact.

©2020 Analog Devices, Inc. All rights reserved. Trademarks and registered trademarks are the property of their respective owners.

VISIT ANALOG.COM

Ask our ADI technology experts tough questions, browse FAQs, or join a conversation at the EngineerZone Online Support Community. Visit ez.analog.com.